

Corrosion Processes of Uranus B6 and Monel 400 Special Alloys in Deep Eutectic Solvents

ELENA IONELA NEACSU¹, VIRGIL CONSTANTIN^{1*}, CRISTINA DONATH¹, KAZIMIR YANUSHKEVICH², ALIONA ZHIVULKA², ANATHOLY GALYAS², OLGA DEMIDENKO², ANA MARIA POPESCU^{1*}

¹ Ilie Murgulescu Institute of Physical Chemistry of the Romanian Academy, Laboratory of Electrochemistry and Corrosion, Splaiul Independentei 202, 060021, Bucharest, Romania

² Scientific Practical Materials Research Centre of NAS Belarus, Laboratory of Physics of Magnetic Materials 19 P. Brovki Str., Minsk, Belarus

The corrosion behaviour of special alloys (Uranus B6 steel and Monel 400) exposed to chlorine chloride-deep eutectic solvents (DES) at 353 K has been investigated by polarization curves method. The corresponding corrosion parameters in choline chloride-oxalic acid and choline chloride-malonic acid were calculated. Micrographic images before and after immersion in the corrosive medium were obtained. Measurements of the influence of the corrosion process on the crystal structure and specific magnetization of the studied steels was carried out by using X-ray diffraction and respectively ponderomotive methods.

Keywords: Corrosion of alloys, Deep Eutectic Solvents, Polarization curves, Micrography, XRD analyses, Magnetization

Recently, ionic liquids (ILs) have been proposed as an alternative solvent to aqueous electrolytes in electrochemical processes such as: deposition of metals and alloys, generation of batteries, catalysis process and organic synthesis [1-4]. Deep eutectic solvents (DESS) belong to the family of ionic liquids. DESS are excellent electrolytes due to characteristics as melting points below 373 K, low toxicity, easy preparation, low vapor pressure, non-flammability and low cost. Generally, DESS are prepared as a mixture composed of a quaternary ammonium salt and a hydrogen bond donor. The melting point of the DESS is lower than their individual components, this decrement being a consequence of the hydrogen bond between halide ion and hydrogen bond donor [5-7].

There are different DESs components, but the most popular is choline chloride (ChCl) which is considered an essential nutrient, biodegradable and non-toxic salt [8]. ChCl is a quaternary ammonium salt which can form eutectic mixtures with very low crystallization temperature with hydrogen bond donors such as carbamide, carboxylic acids and polyols [9,10]. Deep eutectic solvents represent a green and non-expensive substitute for traditional ionic liquids as non-aqueous electrolytes (NAE). Electrochemical applications in NAE benefit from the extended potential windows, due to the absence or minimization of water content. However, interactions between electrode and electrolyte, as well as their degradation, embody a relevant but unexplored territory for the implementation in electrochemical systems. DESS are safe for humans and environment and fulfil all requirements of *green chemistry*.

The vast majority of modern scientific literatures on DESS are dedicated to the investigation of their different properties and practical applications [11-14]. Only very few papers concentrate on metals dissolution [15, 16] and corrosion properties of these solvents [17-19]. However, the corrosion process affects almost all aspects of modern life and the full implementation of ionic liquids, hence it is impossible without knowing how corrosion proceeds.

In the present work is performed a study on the corrosion behaviour of a special stainless steel (Uranus B6) and a nickel-copper alloy (Monel 400) in two different DESs (ChCl-oxalic acid and ChCl-malonic acid), along with the study

of corrosion influence on the structure and magnetic properties of these steels.

Experimental part

Materials and samples preparation

In this study, we investigated two special metallic materials: Uranus B6 and Monel 400. The steel Uranus B6 (ASTM B 625-UNS N08904) is a multipurpose chromium-molybdenum austenitic steel with high corrosion resistance and Monel 400 (ASTM B127-UNS N04400) is a nickel-copper alloy with excellent corrosion resistance in a wide variety of media. The chemical compositions of these materials are: Uranus B6 (20% Cr, 4.3% Mo, 0.02% C, 25% Ni, 0.13% N, Fe balance) and Monel 400 (31% Cu, 2.5% Fe, 2% Mn, 0.5% Si, 0.3% C, 0.024% S, Ni balance). Samples were prepared for corrosion study according to ASTM-G31 standard practice and was presented in a previous paper [20].

Potentiodynamic polarization measurements

Corrosion behavior of the samples was evaluated through potentiodynamic polarization tests in a standard three-electrode cell. The polarization tests were conducted in two DES systems: ChCl-oxalic acid (1:1 molar ratio) and ChCl-malonic acid (1:2 molar ratio) at 353 K, using a Princeton Applied Research, model PARSTAT 2273, potentiostat/galvanostat with a Power Corr software [21].

Both DESs were prepared in our laboratory by mixing the choline chloride (ChCl) with oxalic acid or malonic acid until a homogeneous and colorless liquid was formed [20]. We made no further purification on the reagents used taking in account that water traces in hydrophobic ionic liquid media surprisingly proved to exhibit unusual corrosion inhibiting behavior by protecting copper and nickel under aerobic conditions [22]. The physico-chemical properties (density, viscosity and electrical conductivity) of the used DESs were determined in previous published papers [23,24]. A 1 cm² surface area of the samples was used as the working electrode (WE); the counter electrode was a Pt plate (Radiometer) and a reference electrode Ag/AgCl (0.5 M AgCl Radiometer) was used. All corrosion experiments were performed in a thermostatic glass cell

* emails: virgilconstantin@yahoo.com; popescuamj@yahoo.com

located at a Faraday cage to prevent electrical interferences. To achieve reproducible results, each determination was made three times. The working electrode was maintained in a static position and solutions were aerated. The samples were immersed in the electrolyte before the tests start and were allowed to reach equilibrium, which usually took around 20 min. Polarization curves and open circuit (E_{OCP}) measurements have been used in order to establish the corrosion potential in time. Tafel polarization experiments were performed with a constant scan rate of $0.166 \text{ mV} \times \text{s}^{-1}$, while the potential was shifted within $\pm 250 \text{ mV}$ versus E_{OCP} [25].

Crystal structure, micrographic and magnetic characterization

The crystal structure of metallic samples was characterized by X-ray diffraction (XRD) and the temperature dependence of the specific magnetization was studied in the temperature range of 77-1100 K by the ponderomotive method in the magnetic field of 0.86 Tesla. Details on the both methods was done before [20]. The average size of crystallites (d) was calculated using the Debye-Scherrer equation [26, 27]: $B(2\theta) = k\lambda/d \times \cos\theta$, where k is a constant taken as 0.94, λ is the wavelength of the X-ray radiation (Cu-K α = 0.15406 nm), θ is the diffraction angle and B is the line width at half maximum height (FWHM) [28, 29]. Dislocation density, δ , is determined by equation: $\delta = 1/d^2$.

The micrographic images with x100-x800 magnifications were obtained with a metallurgical microscope (New York Microscope Comp.) with camera acquisition.

Results and discussions

Electrochemical test results

The open circuit potential (OCP) of Uranus B6 and Monel 400 samples is expected to be dependent on the characteristics of resulted oxides, such as oxide thickness, chemical composition, conductivity, structure, etc. After 7-10 min time of immersion at 353 K in the DESs corrosive environment the studied metallic materials present OCP potential values varying from -0.09 V for Uranus B6 to -0.0161 V for Monel400 in ChCl-malonic acid and from 0.027 V for Uranus B6 to 0.075V for Monel 400 in ChCl-oxalic acid. The OCP values are listed in table 1.

Figure 1 shows the Tafel plots obtained from the potentiodynamic polarization curves of the samples in the ChCl-malonic acid. Figure 2 shows the Tafel plots obtained from similar polarization curves of the samples in the ChCl-oxalic acid.

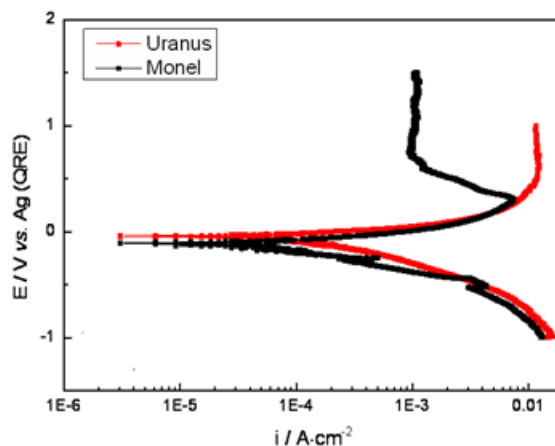


Fig.1 Potentiodynamic polarization curves of Uranus B6 and Monel 400 in ChCl-malonic acid (1:2 molar ratio) at 353 K

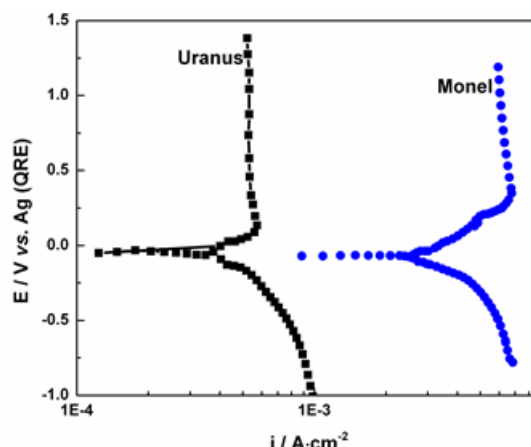


Fig.2 Potentiodynamic polarization curves of Uranus B6 and Monel 400 in ChCl-oxalic acid (1:1 molar ratio) at 353 K

Corrosion potential (E_{corr}) and corrosion current density (i_{corr}) derived from the polarization curves using Tafel slopes extrapolation are summarized in table 1. Corrosion rate (CR) expressed as penetration index in millimeter per year was calculated from equation: $\text{CR} = 87.6 \times i_{\text{corr}} / (\rho \times z \times F)$, where ρ is the density of metallic material (taken approximately $8 \text{ g} \times \text{cm}^{-3}$), $z=2$ number of transferred electrons and F is the Faraday constant. The plots and the corrosion data indicate that all studied materials have good corrosion protective properties with corrosion rates ranging from $0.72\text{-}4.36 \text{ } \mu\text{m}/\text{year}$.

In the ChCl-oxalic acid mixt rates of corrosion for both tested materials are almost same: $0.79 \text{ } \mu\text{m}/\text{year}$ for Uranus B6 and $0.72 \text{ } \mu\text{m}/\text{year}$ for Monel 400. In the ChCl-malonic acid mixture the rates of corrosion are diferent, as it follows: Uranus B6 has the rate of $2.51 \text{ } \mu\text{m}/\text{year}$ and Monel400 has

Table 1
CORROSION PARAMETERS CALCULATED FROM TAFEL PLOTS

| | Sample | E_{OCP} (V) | E_{corr} (V) | i_{corr} ($\mu\text{A}/\text{cm}^2$) | CR ($\mu\text{m}/\text{year}$) |
|-----------------------------|-----------|-------------------------|--------------------------|--|-------------------------------------|
| ChCl-oxalic acid (1:1)M | Uranus B6 | -0.091 | -0.834 | 68.11 | 0.79 |
| | Monel 400 | -0.161 | -0.587 | 67.27 | 0.72 |
| ChCl-malonic acid (1:2)M | Uranus B6 | 0.027 | -0.045 | 214.40 | 2.51 |
| | Monel 400 | 0.075 | -0.110 | 404.70 | 4.36 |

Where: E_{OCP} =rest potential (open circuit potential), E_{corr} =corrosion potential, i_{corr} = corrosion current density, CR=corrosion rate.

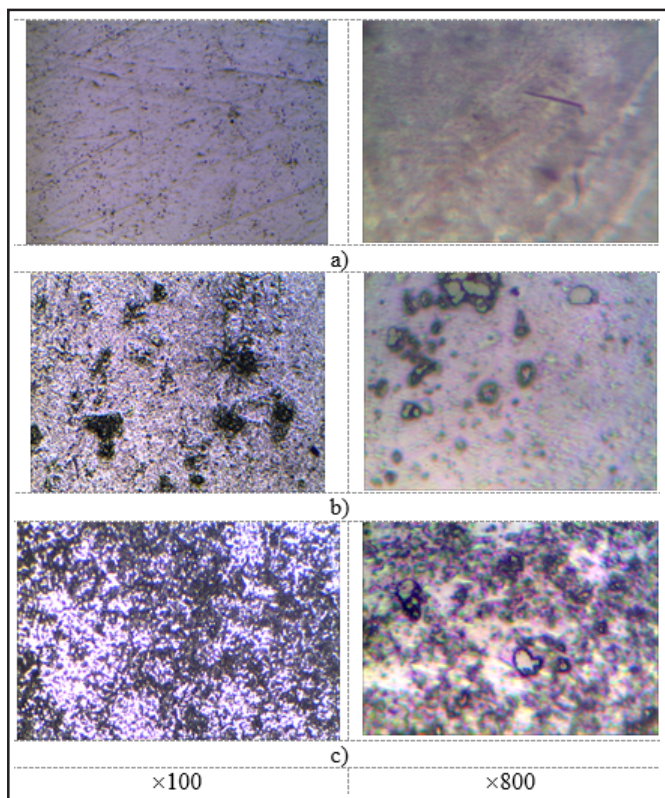


Fig.3 Micrographic image of Uranus B6 sample: a) initial stage; b) corroded in ChCl-oxalic acid; c) corroded in ChCl-malonic acid

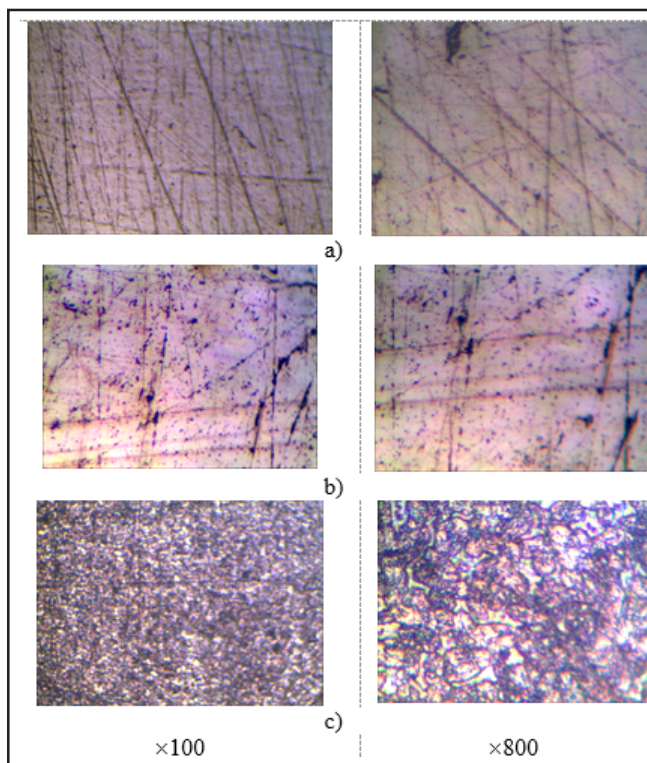


Fig.4 Micrographic image of Monel 400 sample: a) initial stage; b) corroded in ChCl-oxalic acid; c) corroded in ChCl-malonic acid

the rate of $4.36 \mu\text{m}/\text{year}$. We can see that in this DES the rates of corrosion are grown (bigger), which indicates that this mixture presents aggressivity at corrosion. Both metallic samples have the lowest corrosion rate in ChCl-Oxalic acid, so it can be said that the passive layer formed on their surface is more stable and resistant. Regarding the aggressiveness of the electrolytes we can mention that the ChCl- malonic acid mixture is much more aggressive.

Microscopic study

Microscopic images in figure 3 show that Uranus B6 steel has a compact and homogeneous surface before corrosion and after corrosion the surface of that sample shows some changes due to the corrosiveness of DESs. Microscopic images in figure 4 show that Monel 400 alloy also has a compact and homogeneous surface before corrosion and after corrosion the surface of that sample shows some changes.

The microscopic images show also that for both samples Uranus B6 and Monel 400 the corrosion in ChCl-oxalic acid is stronger.

XRD analysis for crystal structure

On figure 5 are presented X-ray patterns of Uranus B6 sample before and after corrosion action of the ChCl-oxalic acid (1:1 M) and ChCl-malonic acid (1:2 M). On figure 6 is shown more detailed part of this pattern. It is revealed that for Uranus B6 the main phase FeNi (Fm3m sp.gr.) is saved.

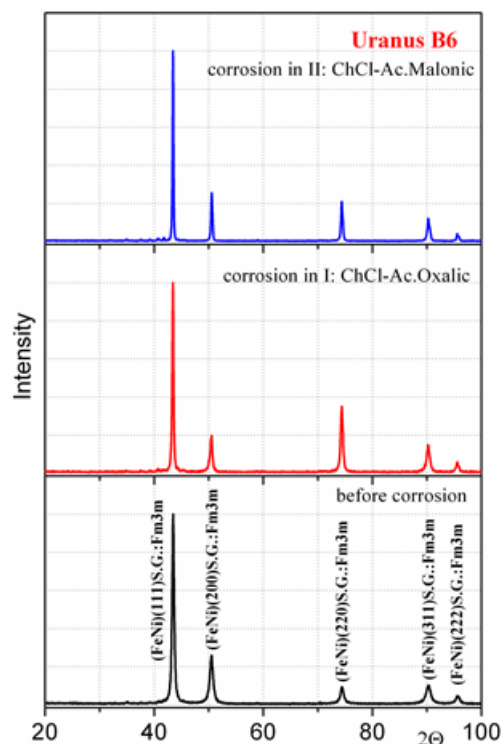


Fig.5 XRD-Analysis of Uranus B6 sample before and after corrosion in DES.

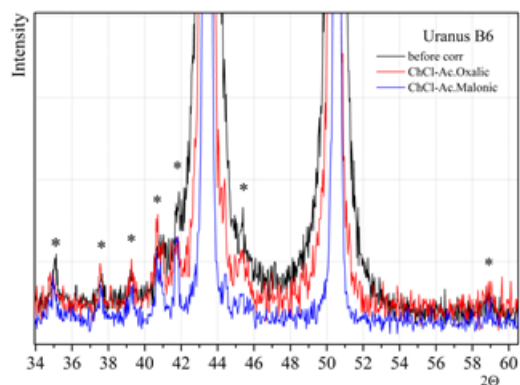


Fig.6 Detailed X-ray patterns before and after corrosion action of DES for Uranus B6

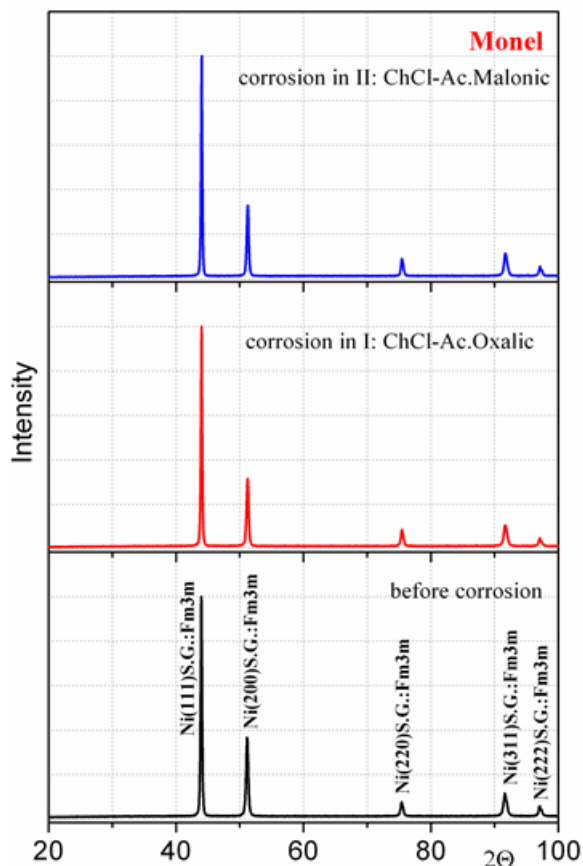


Fig. 7 XRD-Analysis of Monel 400 sample before and after corrosion

The presence of reflexes marked by (*) on figure 6 may be caused by oxides impurity. The analysis of other X-ray patterns (fig.7) showed that Monel 400 has a nickel based alloy structure with a cubic unit cell of Fm3m space group. After corrosion action of ChCl-malonic acid and ChCl-oxalic acid no extra Bragg reflexes are observed on X-ray patterns of both studied samples that indicates no changes of crystal structure, and the corrosion action does not has a significant influence. The crystal parameters of investigated samples before and after corrosion action are presented in table 2.

Magnetic properties

The temperature dependences of the specific magnetization $\sigma = f(T)$ of Uranus B6 and Monel 400 (dependences $\sigma^2 = f(T)$ in inserts) are presented in figure 8. Uranus B6 is almost non-magnetic. At liquid nitrogen temperature the value of σ is only $4.11 \text{ A}\cdot\text{m}^2\cdot\text{kg}^{-1}$, and the Curie temperature is 185 K. Monel has low specific magnetization value, $26.5 \text{ A}\cdot\text{m}^2\cdot\text{kg}^{-1}$ at liquid nitrogen temperature and at room temperatures it becomes paramagnetic (fig. 1, a). It is revealed that the slow cooling leads to decreasing of the specific magnetization to a value about $28.0 \text{ A}\cdot\text{m}^2\cdot\text{kg}^{-1}$ at liquid nitrogen temperature and Curie temperature to 310 K. This fact can be caused by sample annealing.

On figure 9 is shown the comparison of specific magnetization dependences (σ) for Monel 400 and Uranus B6 before and after corrosion action of DESs during heating. The corrosive action of ChCl-malonic acid and ChCl-oxalic acid deep eutectic solvents has only surface influence and hasn't significant effect on specific magnetization values of these samples. The parameters of curves are presented in table 3. For both samples it is also observed a decrease of specific magnetization during slow cooling up to liquid nitrogen temperature.

Table 2
CRYSTAL PARAMETERS FOR URANUS B6 AND MONEL 400

| Sample | a, nm | Average size of crystallites $\delta \cdot 10^{-3}, \text{ nm}^{-2}$ |
|--|--------|--|
| Monel 400 before corrosion | 0.3566 | 20.71 |
| Monel 400 in ChCl-oxalic acid (1:1 molar ratio) | 0.3565 | 21.75 |
| Monel 400 in ChCl-malonic acid (1:2 molar ratio) | 0.3565 | 21.72 |
| Uranus B6 before corrosion | 0.3607 | 13.04 |
| Uranus B6 in ChCl-oxalic acid (1:1 molar ratio) | 0.3609 | 18.99 |
| Uranus B6 in ChCl-malonic acid (1:2 molar ratio) | 0.3609 | 18.84 |

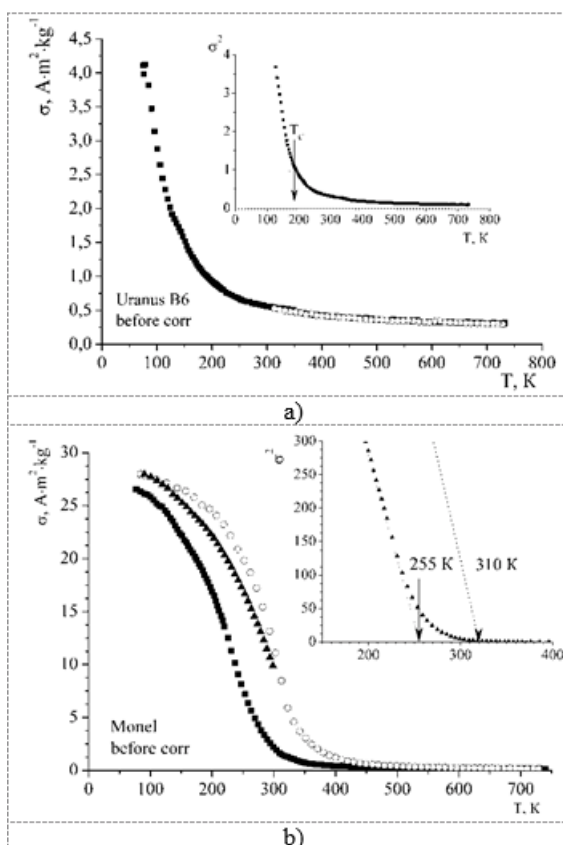


fig. 8. temperature dependences of the specific magnetization of a) Uranus B6 and b) Monel 400 (■ -heating; ○-cooling; ▲-heating 2)

Table 3
MAGNETIC PARAMETRS OF URANUS B6 AND MONEL 400

| Sample | $\sigma, \text{ A}\cdot\text{m}^2\cdot\text{kg}^{-1}$ | $T_c, \text{ K}$ |
|--|---|------------------|
| Uranus B6 before corrosion | 4.11 | 185 |
| Uranus B6 in ChCl-oxalic acid (1:1 molar ratio) | 4.76 | 200 |
| Uranus B6 in ChCl-malonic acid (1:2 molar ratio) | 4.72 | 200 |
| Monel 400 before corrosion | 26.5 | 255 |
| Monel 400 in ChCl-oxalic acid (1:1 molar ratio) | 26 | 265 |
| Monel 400 in ChCl-malonic acid (1:2 molar ratio) | 21.7 | 260 |

Conclusions

The study of crystal structure and specific magnetization of Uranus B6 and Monel 400 metallic materials before and after corrosion action of ChCl-malonic acid (1:2 molar ratio) and ChCl-oxalic acid (1:1 molar ratio) deep eutectic solvents was successfully carried out. XRD data confirm that the main phase of Uranus B6 is FeNi (Fm3m sp.gr.) while for Monel 400 is a nickel based alloy with a structure as a cubic unit cell of Fm3m space group. Uranus B6 and Monel 400 have a low specific magnetization value and a phase transition temperatures of 255 and 185 K. Both of these samples are heating resistant up to 1100 K. It was revealed, that corrosion action of DES (ChCl-malonic acid or ChCl-oxalic acid) does not have a significant effect on the crystal structure and specific magnetic characteristics. However in the ChCl-oxalic acid these materials behave better and they have a less rate of corrosion than in ChCl-malonic acid. The alloys also present transpassivation in both DESs. Consequently, it may be considered that the alloy tested are safe to use as construction materials for the components which are in direct contact with the ionic liquids and deep eutectic solvents.

Acknowledgement: The work was carried out within the programm: Electrode processes, materials for electrochemical processes and corrosion of the Institute of Physical Chemistry and was supported by the Romanian Academy and the Academy of Sciences of the Republic of Belarus Foundation for Basic Research (project 2016-2017). Authors equally contributed to this work.

References

1. SHU-I, H., JING-FANG, H., I-WEN, S., CHENG-HUI, Y., SHIEA, J., *Electrochim. Acta.*, **47**, 2002, p. 4367.
2. ABBOTT, A.P., BARRON, J.C., RYDER, K.S., WILSON, D., *Chem. Eur. J.*, **13**, 2007, p. 6495.
3. DILASARI, B., JUNG, Y., KWON, K., *Electrochem. Commun.*, **73**, 2016, p. 20.
4. BAKKAR, A., NEUBERT, V., *Electrochem. Commun.*, **51**, p. 113.
5. SMITH, E. L., ABBOTT, A. P., RYDER, K. S., *Chem. Rev.*, **114**, 2014, p.11060.
6. PRATHISH, K.P., CARVALHO, R.C., BRET, M.A., *Electrochem. Commun.*, **44**, 2014, p. 8.
7. RU, J., HUA, Y., XU, C., LI, J., LI, Y., WANG, D., ZHOU, Z., GONG, K., *Appl. Surf. Sci.*, **357**, 2015, p. 2094.

8. ABO-HAMAD, A., HAYYAN, M., ALSAADI, M.A., HASHIM, A., *Chem. Eng. J.*, **273**, 2015, p. 551.
9. ABBOTT, A.P., CAPPER, G., DAVIES, D.L., MCKENZIE, K.J., OBI, S.U., *J. Chem. Eng. Data*, **51**, 2006, p. 1280.
10. PROTSENKO, V.S., KITKYK, A., SHAIDEROV, A., DANILOV, F.I., *J. Molecular Liquids*, **212**, 2015, p. 716.
11. SMITH, E.L., ABBOTT, A.P., RYDET, K.S., *Chem. Rev.*, **114**, 2014, p. 11060.
12. MBOUS, Y.P., HAYYAN, M., HAYYAN, A., WONG, W.F., HASHIM, M.A., LOOI, C.Y., *Biotechnol. Adv.*, **35**, 2017, p. 105.
13. POPESCU, A.M., CONSTANTIN, V., *Chem. Res. Chinese Univ.*, **30**, 2014, p. 119.
14. POPESCU, A.M., CONSTANTIN, V., COJOCARU, A., OLTEANU, M., *Rev.Chim.(Bucharest)*, **62**, 2011, p. 206.
15. ABBOTT, A.P., FRISCH, G., HARTLEY, J., KARIM, W.O., RYDER, K.S., *Progress in Natural Science*, **25**, 2015, p. 595.
16. ABBASA, Q., BINDERB, L., *ECS Trans*, **33**, 2011, p. 57.
17. GREEN, T.A., VALVERDE, P., ROY, S., *J. Electrochem. Sci.*, **165.**, 2018, p. 313.
18. KITKYKA, A.A., RUDLOVVA, Y. D., KELMB, A., MALYSHEVB, V.V., BANNYKA, N.G., KABULSKAC, I.F., *J. Electroanal. Chem.*, **823**, 2018, p. 234.
19. GUTIERREZ, E., RODRIGUEZ, J.A., BORBOLLA, J.C., CASTRILLEJO, E.B., *Int. J. Electrochem. Sci.*, **13**, 2018, p. 11016.
20. NEACSU, E.I., CONSTANTIN, V., DONATH, C., YANUSHEKEVICH, ZHIVULKA, GALYAS, A., DEMIDENKO, O., POPESCU, A.M., *Rev.Chim. (Bucharest)*, **69**, no. 2018, 10, p. 2642.
21. NEACSU, E.I., CONSTANTIN, V., SOARE, V., OSICEANU, P., POPA, M.V., POPESCU, A.M., *Rev. Chim. (Bucharest)*, **64**, 2013, p. 994.
22. LEBEDEVA, O., JUNGUROVA, G., ZAKHAROV, A, KULTIN, D., CHERNIKOVA, E., KUSTOV, L., *J. Phys. Chem. C*, **116**, 2012, p. 22526.
23. POPESCU, A.M., CONSTANTIN, V., FLOREA, A., BARAN, A., *Rev.Chim. (Bucharest)*, **62**, 2011, p. 5310.
24. POPESCU, A.M., DONATH, C., CONSTANTIN, V., *Bulg. Chem. Commun.*, **46**, 2014, p. 452.
25. KRUGER, J., Chapter 12 in *Uhlig's Corrosion Handbook*, 3-rd ed, John Wiley & Sons Inc, Hoboken, NJ, USA, 2011.
26. SCHERRER, P., *Nachr. Ges. Wiss. Göttingen*, **26**, 1918, p. 98.
27. LANGFORD, J.L., WILSON, A.J.C., *J. Appl. Cryst.*, **11**, 1978, p. 102.
28. LANGFORD, J.L., WILSON, A.J.C., *J. Appl. Cryst.*, **11**, 1978, p. 102.
29. BARAKAT, M.A., HAYES, G., ISMAT SHAH, S., *J. Nanosci. Nanotechnol.*, **5**, 2005, p. 759.

Manuscript received: 19.12.2018